MORPHOLOGICAL, STRUCTURAL AND OPTICAL CHARACTERISTICS OF ZNIC OXIDE GROWN BY CHEMICAL BATH DEPOSITION METHOD

LUO YEXING

UNIVERSITI SAINS MALAYSIA

2025

MORPHOLOGICAL, STRUCTURAL AND OPTICAL CHARACTERISTICS OF ZINC OXIDE GROWN BY CHEMICAL BATH DEPOSITION METHOD

by

LUO YEXING

Thesis submitted in fulfilment of the requirements
for the degree of
Master of Science

September 2025

ACKNOWLEDGEMENT

I would like to express my sincerest gratitude to all those who have helped me throughout this project and my postgraduate career.

First and foremost, I would like to express my strong and heartfelt appreciation to my research supervisor, Assoc. Prof. Dr. Yam Fong Kwong, for his guidance throughout this research. I am honoured to have met such a wonderful supervisor and to be able to study under his guidance. During the whole research period, he not only provided me with experimental ideas but also shared his professional knowledge with me without any hesitation and often pushed me to study hard. As I am a foreigner, he also cares about whether I am used to living in Malaysia. His kindness, vision, and sincerity encouraged me deeply, and without his support and motivation, this thesis would not have been completed.

In addition, I would like to send my thanks to the two Drs of lab 335, Dr. Beh Khi Poay and Dr. Ahmad Umar Ahmad, for their help in teaching me how to use the equipment and sharing their knowledge with me. I would also like to thank my senior Samuel Obaseki and Feng Taixiang for their kind help, helping me to get familiar with the environment and the lab equipment as soon as possible. I would also like to thank my fellow graduate student partner, Lim Jieh Sim, for mutual support and academic discussions throughout the research. I would also like to thank all the staff in the photonics lab for their assistance in experiments and troubleshooting. Thanks to their help, I was able to get good experimental data.

Finally, I am deeply thankful to my family, especially my mother, for their unwavering care and encouragement, which gave me the strength to complete my master's degree abroad.

TABLE OF CONTENTS

LIST OF TABLES

Page

LIST OF FIGURES

Page

LIST OF SYMBOLS

A	Absorbance
C	lattice constant
C_0	Unstrained lattice constant
D	Average crystallite size
d	Interplanar spacing of the crystal lattice in Bragg's law
E_g	Optical bandgap energy
h	Planck constant
K	Scherrer constant
l	(00l) plane
n	Refractive index
n_s	Refractive index of the substrate
T_M	Upper envelope, maximum
T_m	Lower envelope, minimum
T_s	Transmittance of the substrate
t	Thickness obtained by Swanepoel method
Δ	Phase change
Ψ	Amplitude ratio
α	Absorption coefficient
β	Full width half maximum
ε_{zz}	Lattice strain percentage
θ	Angle between the incident X-ray and crystal plane
λ	Wavelength
υ	Velocity of light

LIST OF ABBREVIATIONS

1D	One-dimensional
ALD	Atomic layer deposition
AZO	Aluminum doped zinc oxide
CBD	Chemical bath deposition
DI	Deionized
EDX	Energy dispersive X-ray
EMA	Effective medium approximation
FESEM	Field emission scanning electron microscopy
FWHM	Full width half maximum
HMTA	Hexamethylenetetramine
ITO	Indium tin oxide
IZO	Indium doped zinc oxide
MR	Methyl Red
MwPA	Microwave plasma annealing
PLD	Pulsed laser deposition
PL	Photoluminescence
pH	Potential of hydrogen
PVA	Polyvinyl alcohol
RF	Radio-frequency
SEM	Scanning electron microscope
SE	Spectroscope ellipsometry
SPT	Spray pyrolysis technique
TA	Temperature annealing
UV-Vis	Ultraviolet-visible
UV	Ultraviolet
XRD	X-ray diffraction
ZnO	Zinc oxide

LIST OF APPENDICES

CIRI-CIRI MORFOLOGI, STRUKTUR DAN OPTIK ZINK OKSIDA DITUMBUH DENGAN KAEDAH PEMENDAPAN MANDIAN KIMIA

ABSTRAK

Projek ini adalah untuk menyiasat sifat morfologi, struktur dan optik filem nipis Zink oksida (ZnO) yang ditumbuh pada kaca sebagai substrat melalui kaedah pemendapan mandi kimia (CBD) dengan tempoh yang berbeza. Dalam kerja ini, serbuk hexamethylenetetramine (HMTA, $C_6H_{12}N_4$) dan zink nitrat heksahidrat ($Zn(NO_3)_2$-$6H_2O$) dicampur dengan nisbah molar 1:1 dan dilarutkan dalam air ternyahion (DI) untuk menjadikan larutan prekursor yang diperlukan untuk pertumbuhan ZnO. Sebelum pertumbuhan CBD, lapisan benih ZnO mula-mula diendapkan oleh magnetron frekuensi radio (RF) yang terpercik pada semua substrat kaca supaya ZnO yang sejajar boleh diperolehi. Siri sampel ini diperoleh dengan mengubah masa pertumbuhan, iaitu 0.5, 1, 2, dan 4 jam. Keadaan pertumbuhan lain telah ditetapkan pada kepekatan larutan 0.1 M dan suhu 80°C. Sifat-sifat filem ZnO telah dikaji oleh mikroskop elektron pengimbasan pancaran medan (FESEM), pembelauan sinar-X (XRD), dan spektrofotometer ultraungu-kelihatan (UV-Vis). Pengukuran FESEM menunjukkan bahawa semua filem terdiri daripada nanorod ZnO yang homogen dan sejajar. Ketebalan filem meningkat daripada 466.7 kepada 1297.0 nm dan diameter struktur nano ZnO meningkat dengan tempoh CBD daripada 103.7 kepada 325.7 nm. Keputusan XRD menunjukkan bahawa semua filem ZnO mempunyai puncak dominan sengit dan tajam (002) dan puncak (004) yang merupakan puncak pantulan sekunder dari (002), ini menunjukkan bahawa siri sampel ini mempunyai kualiti kristal yang baik. Jurang jalur optik seperti yang diperoleh daripada ukuran UV-Vis didapati di antara 3.36 hingga 3.40 eV. Untuk penentuan

indeks biasan dan ketebalan optik filem ZnO, kaedah Swanepoel juga telah digunakan. Indeks biasan meningkat dengan panjang gelombang dari 300 hingga 1400 nm. Nilai ketebalan optik dari 529.1 hingga 1304.9 nm dikira dengan kaedah Swanepoel, menunjukkan persetujuan yang baik dengan ketebalan fizikal yang diukur oleh FESEM.

MORPHOLOGICAL, STRUCTURAL AND OPTICAL CHARACTERISTICS OF ZINC OXIDE GROWN BY CHEMICAL BATH DEPOSITION METHOD

ABSTRACT

This project is to investigate the morphological, structural and optical properties of Zinc oxide (ZnO) thin films grown on glass as the substrate by chemical bath deposition (CBD) method with different durations. In this work, hexamethylenetetramine (HMTA, $C_6H_{12}N_4$) and zinc nitrate hexahydrate ($Zn(NO_3)_2$-$6H_2O$) powder were mixed with 1:1 molar ratio and dissolved in deionized (DI) water to make the precursor solution required for the growth of ZnO. Prior to the CBD growth, a ZnO seed layer was first deposited by radio-frequency (RF) magnetron sputtering on all the glass substrates so that well-aligned ZnO could be obtained. This series of samples was obtained by varying the growth time, which was 0.5, 1, 2, and 4 h. The other growth conditions were fixed at a 0.1 M solution concentration and temperature of 80°C. The properties of ZnO films have been studied by the field-emission scanning electron microscopy (FESEM), X-ray diffraction (XRD), and ultraviolet-visible spectrophotometer (UV-Vis). The FESEM measurements demonstrate that all the films consist of homogeneous and well-aligned ZnO nanorods. The film thickness increases from 466.7 to 1297.0 nm and the diameter of the ZnO nanostructure rises with CBD duration from 103.7 to 325.7 nm. The XRD results show that all the ZnO films have intense and sharp (002) dominant peak and (004) peak which is the secondary reflection peak from (002), indicating that this series of samples have good crystal quality. Optical bandgap as derived from UV-Vis measurements is found to be ranging from 3.36 to 3.40 eV. For the determination of the refractive index and optical thickness of ZnO films, the Swanepoel method has also been employed.

The refractive index increases with wavelength from 300 to 1400 nm. The optical thickness values from 529.1 to 1304.9 nm were calculated by the Swanepoel method, showing good agreement with the physical thickness measured by FESEM.

INTRODUCTION

1.1 Introduction of ZnO

ZnO is a semiconductor with great research potential due to its wide direct bandgap (3.37 eV) and large exciton binding energy (60 mV), which has encouraged many researchers to investigate its unique properties. Because of its extraordinary electrical and optical absorption properties, zinc oxide is widely used in optoelectronic devices, such as solar cells, photodetectors, light-emitting diodes, etc.(Xu & Wang, 2011). ZnO, as a compound semiconductor of group II-IV, has an ionicity intermediate between that of covalent semiconductors and ionic semiconductors. In zinc oxide, the Zn^{2+} is coordinated to the $6O^{2-}$, and because of the sp^3 hybridization of electronic states involved in the Zn-O bond, the Zn^{2+} takes position at the tetrahedral site. Based on first-principles calculations, it has been found that there is a strong Coulomb repulsion between Zn and O due to the filled M shell outside the nucleus of the Zn atom, which drives the Zn ion to move towards the O ion. Since the bonding geometry of the tetrahedral coordination determines the crystal structure of ZnO, different crystal structures of ZnO can be synthesized depending on the growth conditions: e.g., wurtzite, zinc blende, and rock salt (T.-T. Fang, 2018). In general, the wurtzite phase (hexagonal crystal system) is the most stable under ordinary conditions (Gohil & Choudhury, 2019).

ZnO is available in many different nanostructures such as nanowires, nanorods, nanobelts, and nanoflowers (Clarke & Ghandi, 2023). They are one-dimensional (1D) nanostructures that exhibit high thermal and mechanical stability and also have excellent properties such as high mobility carrier transport, efficient light confinement, and light emission. Therefore, 1D ZnO nanomaterials are often considered an optimal

medium for the construction of optoelectronic devices, which can improve the performance of optoelectronic devices(Kwok, 2019)(M. Ding et al., 2018). Different nanostructures of ZnO have their individual properties and can be obtained by different processing methods.

There are a variety of methods for synthesizing 1D ZnO nanomaterials, such as vapor phase transport, chemical bath deposition (CBD), electrodeposition, chemical vapor deposition (CVD), magnetron sputtering, etc.(Shahzad et al., 2021). Each fabrication method has its specific advantages and unavoidable weaknesses, for example, the gas vapor method of depositing ZnO usually requires high temperatures exceeding 450℃, which limits the choice of substrate and has strict demands on the sealed environment of the gas. Solution deposition is one of the commonly employed methods to obtain 1D ZnO nanostructures because of its low cost, availability at low temperatures as well as controllable processing. The CBD method is one of the solution deposition methods, which is used to induce ZnO nanostructures in a wide scope and can successfully grow well-aligned ZnO. The ZnO structure obtained by CBD is a hexagonal wurtzite structure, which is similar to the one obtained by RF magnetron sputtering.

1.2 Introduction of Swanepoel method

The Swanepoel (Swanepoel, 1983) is a method of simulating wave-like patterns in transmission spectra with smooth curves, which allows the optical constants of semiconductor films to be calculated using a few known equations and has been widely used by many researchers to investigate the optical properties of thin films. The advantage is that the reflectance of the sample is not required for the calculation of the optical parameters, reducing the error in the calculation caused by the reflectance

(Dorranian et al., 2012). It is also possible to calculate the thickness of the film using the Swanepoel method, which leaves the film untouched, unlike mechanical measurements that tend to damage the surface of the film.

1.3 Problem Statement

ZnO has received enormous attention from researchers as a semiconductor with outstanding optical and electrical properties and is one of the materials of choice for optoelectronic device applications. It is important to learn about the optical and structural properties of ZnO as it has broad applicability in the analysis and design of optical and optoelectronic devices. A thorough understanding of the growth mechanism of the target material is required to obtain the desired nanostructures.

a) The CBD method is one of the common methods to grow and synthesise ZnO nanostructures with easy control of the growth parameters. The growth time, on the other hand, is a parameter that plays an important role in the growth process of ZnO nanostructures. The growth and properties of ZnO nanostructures can be varied by changing the duration of CBD. For example, R. A. Rahman et.al reported that the length of the ZnO nanorods became longer with the growth time; the crystallinity of the ZnO increased with longer growth time; and the optical bandgap values of ZnO grown at different times ranging from 3.31 to 3.40 eV (Rahman et al., 2019). The ability to control the thickness and properties of the film by varying the growth time is essential for predicting device behaviour and designing modern optoelectronic devices based on ZnO films.

b) Furthermore, film thickness itself is a crucial parameter strongly influencing ZnO film properties, such as optical bandgap (E_g). R.E. Marotti et al. reported that the bandgap energy of ZnO films shows an increase trend with increasing thickness

(Marotti et al., 2004). A clear understanding of how CBD growth time affects ZnO thin film characteristics (morphology, structure, optics) and its relationship with resulting film thickness is essential for tailoring films for specific optoelectronic device applications, yet remains insufficiently explored. There are different methods for measuring the thickness of ZnO films, among them mechanical methods such as stylus profilometry and interferometry, which require removing a part of the films. For maintaining the integrity of the film surface, it is preferable to choose methods that are non-contact and non-destructive, such as FESEM measurements and the Swanepoel method. Spectroscope ellipsometry (SE) is a common method for measuring the refractive index of thin films, but the formulas involved are too complex and lengthy and need computer models for fitting. The wave-like patterns that appear in reflection and transmission spectra are usually a source of error in the calculation of optical parameters of thin films, and the Swanepoel method can eliminate the effect of this error. Further, the optical bandgap energy (E_g) and refractive index (n) of materials are important factors that affect its optical properties since the optical bandgap and refractive index of the material are directly related to its photosensitivity.

Hence the selection of suitable methods for growing ZnO thin film structures as well as measuring and analysing their structural properties and optical characteristics play a key role in their successful application in optoelectronic devices.

1.4 Originality

Many reports have investigated the effects of varying the experimental parameters used in the CBD method, including precursor concentration, solution pH, substrate selection, seed layer thickness, growth time, and temperature, but focusing on how to analyze the morphological, structural and optical properties variations in

ZnO thin films is relatively novel. It was found that little focus has been placed on the study of the relevance of the optical properties of ZnO films to their process conditions, where the Swanepoel method is a methodology to determine the optical parameters of the films from transmission spectra with interference effects. Therefore, in this work, the influence of CBD growth time on the morphological, structural, and optical properties of ZnO thin films was investigated, presenting how to calculate the refractive index and optical thickness of the films by the Swanepoel method and compare it with the physical thickness measured by FESEM.

1.5 Objectives

In total, this work has the following two research objectives:

a) To investigate the influence of CBD growth time on the morphological, structural and optical properties of ZnO thin films.

b) To determine the refractive index and optical thickness of the films by the Swanepoel method and compare the thickness measured by FESEM and obtained by the Swanepoel method.

1.6 Outline of Thesis

This thesis is divided into six chapters. The first chapter simply introduces the structural properties of zinc oxide and its application in optoelectronic devices, as well as the common fabrication methods for zinc oxide, as well as a short mention of the Swanepoel method. This chapter includes the organization of this thesis and brief contents of each chapter.

Chapter 2 reviews and summarizes the results of studies by other researchers related to the topic of this project. This chapter consists of three parts. The first part reviews

the literature on the related experiments of growing ZnO by CBD method and analyzes the influence of different parameters of CBD on the properties of ZnO. The second part details the methods of measuring thickness and the previous work done by others. The third part state the methods of determining refractive index of thin films, especially for Swanepoel method.

Chapter 3 introduces the sample fabrication method, experimental parameter settings for CBD, and the used materials. And also explains the types of equipment used to characterize the ZnO nanostructures and their working principles.

Chapter 4 analyses the effect of the growth time of CBD on the morphological, structural and optical properties of the samples and further explanation and discussion.

Chapter 5 summarizes the whole thesis and gives suggestions and an outlook for future work.

Chapter 6 lists all the references used in this thesis.

LITERATURE REVIEW

2.1 Introduction

This chapter is broadly divided into two parts. The first part reviews the relevant literature on the synthesis of ZnO nanostructures using the CBD method, discussing the influence of various parameters in the CBD process on morphological, structural and optical properties of ZnO thin films, especially for the effect of deposition duration. The second part outlines the various methods employed for determining the refractive index of thin films, focusing on the fundamental principles of the Swanepoel method and reviewing the relevant literature.

2.2 Chemical Bath Deposition

Thin film deposition process is one of the essential steps in many device fabrication techniques. CBD is a facile and common method of depositing semiconductor thin films by using aqueous precursor solutions, as the process is easy to handle, the equipment used is basic, the cost is low, and it is also possible to deposit thin films over a large surface area at low temperatures, as well as being a reliable technique of production.

The mechanism of CBD can be largely explained as follows: the soluble salts of the required metallic elements are dissolved in aqueous solution, releasing the metal cations; the non-metallic elements are supplied by a suitable source compound, which is decomposed in the presence of hydroxide ions, the anions from the decomposition combined with the cations to form the compounds (Ezekoye, B.A. *et al.*, 2012). In the deposition of zinc oxide thin films by the CBD method, the source of OH^- ions is usually hexamethylenetetramine (HMTA), and Zn^{2+} ions are usually supplied by this kind of zinc compounds, such as zinc sulfate, zinc nitrate, etc. The deposition of thin films by

the CBD method is divided into two steps, the first step is nucleation, and the second step is crystal growth. The above steps require the substrate to be immersed in the solution to take place.

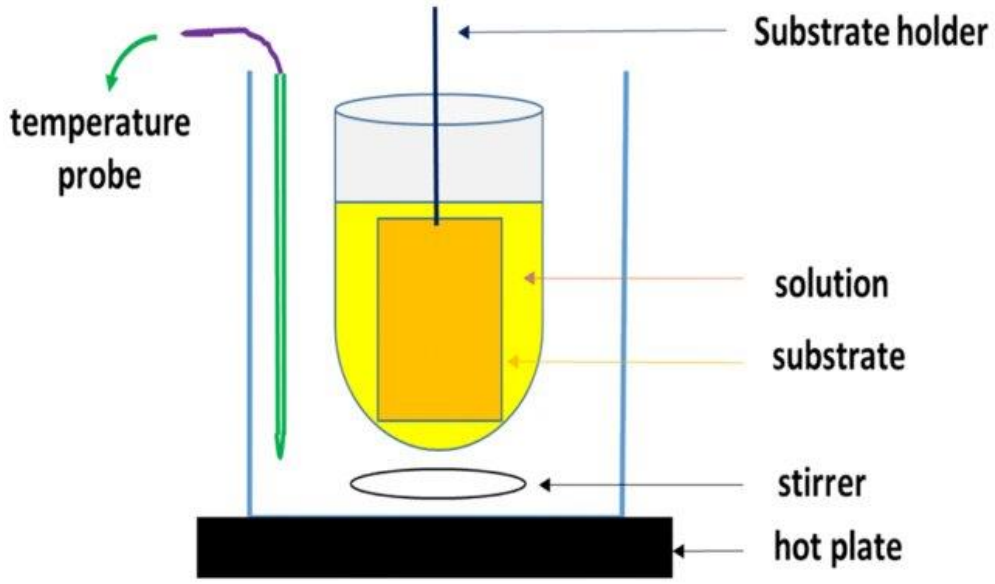

Figure 2.1 Schematic diagram of chemical bath deposition. (Ezekoye, B.A. et al., 2012)

The growth results such as the thickness of the film, crystallite size, shape, and orientation are vital prerequisites for being well applied in optoelectronics and other devices. The morphology of the film is directly affected by the experimental conditions which can be controlled by varying the parameters such as growth temperature, growth duration, solution concentration, pH value and others.

Z.H Zheng et al. reported the growth of ZnO nanorods on ITO substrates by CBD method to investigate the effect of growth time on the optical properties of ZnO nanorods (Zheng et al., 2018). The ZnO seed layer was obtained by the pure zinc acetate solution method. The aqueous solution for growing ZnO nanorods was prepared by mixing zinc nitrate hydrate and hexamethylenetetramine dissolved in deionized water at a molar ratio of 1:1. The solution temperature was maintained at 93°C during growth period, and the reaction times were set at 0.5, 1, 2.5, and 3 h, respectively. Figure 2.2

shows the XRD patterns of ZnO with different growth times. It can be seen that all the samples have hexagonal wurtzite structure and all of them are highly C-axis oriented. The intensity of the (002) plane diffraction peaks increase with the growth time, which indicates that the crystal quality becomes better.

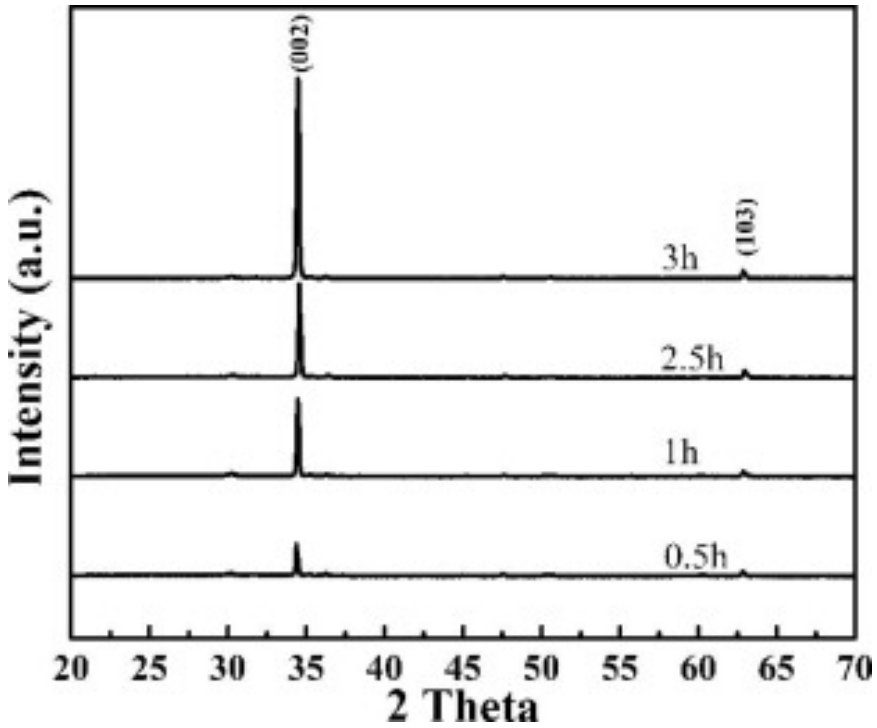

Figure 2.2 XRD patterns of samples obtained at different growth times. (Zheng et al., 2018)

Figure 2.3 shows SEM images of ZnO NRs grown with different deposition times. From all the SEM images it can be seen that the density and uniformity of the distribution of ZnO nanorods were almost invariable. The authors observed that the shape of nanorod tops changed with growth time, transitioning from tapered to flattened, which formed flat (002) crystal plane. This indicates that the characteristics of hexagonal crystals of ZnO nanorods get more and more obvious, consistent with the results obtained from the XRD patterns. In addition, the diameter of ZnO nanorods varies from 36 nm to 155 nm with the increase of growth time. The above results illustrate that the morphology of ZnO thin films can be controlled by adjusting the

growth duration, which can be elucidated by the theory of crystal nucleation and growth: c-axis orientation growth can be attributed to the fact that the (0001) basal plane of hexagonal rods is polar and has relatively high surface energy. Therefore, the growth rate R(0001) is maximum so that larger diameter and longer length ZnO nanorods can be obtained with increasing growth time.

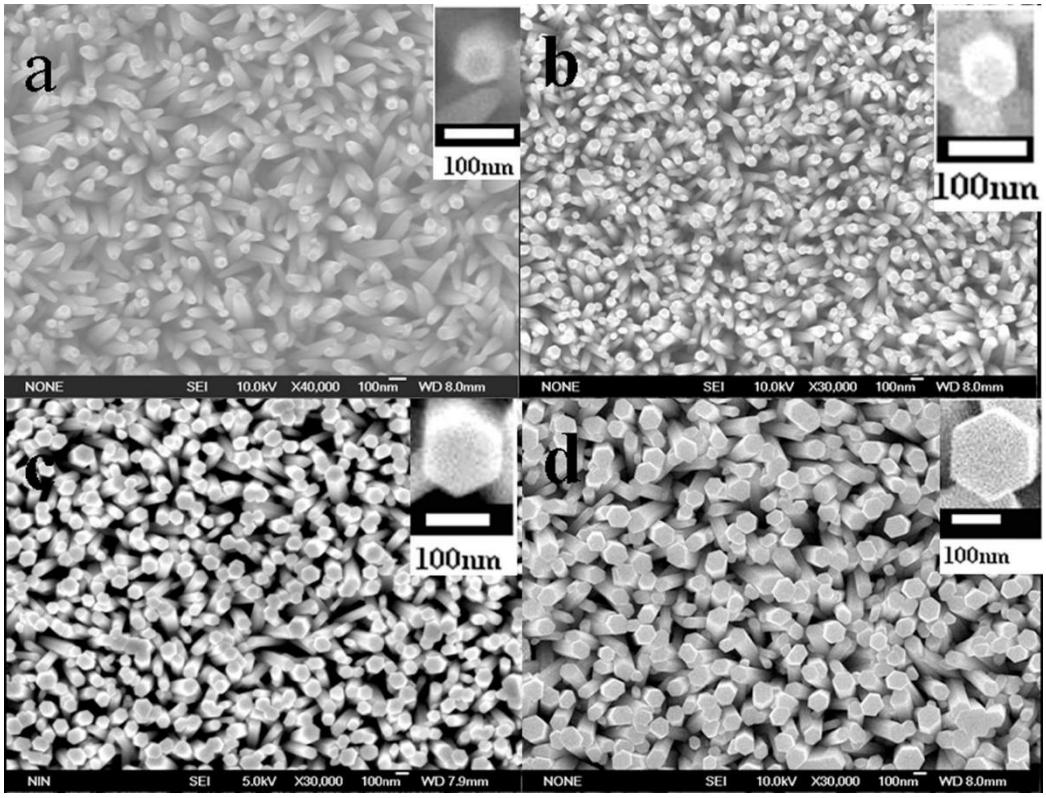

Figure 2.3 SEM images of ZnO nanorods grown on ITO substrate with different growth times. (a) 0.5 h; (b) 1 h; (c) 2.5 h; (d) 3 h. (Zheng et al., 2018)

From the transmission spectra graph of Figure 2.4, the transmittance of all the samples shows a sharp absorption edge in the UV region at 375 nm. Also, the transmittance decreases from 74% to 18% at 600 nm for the samples with growth time increase, which is due to the increase in sample thickness.

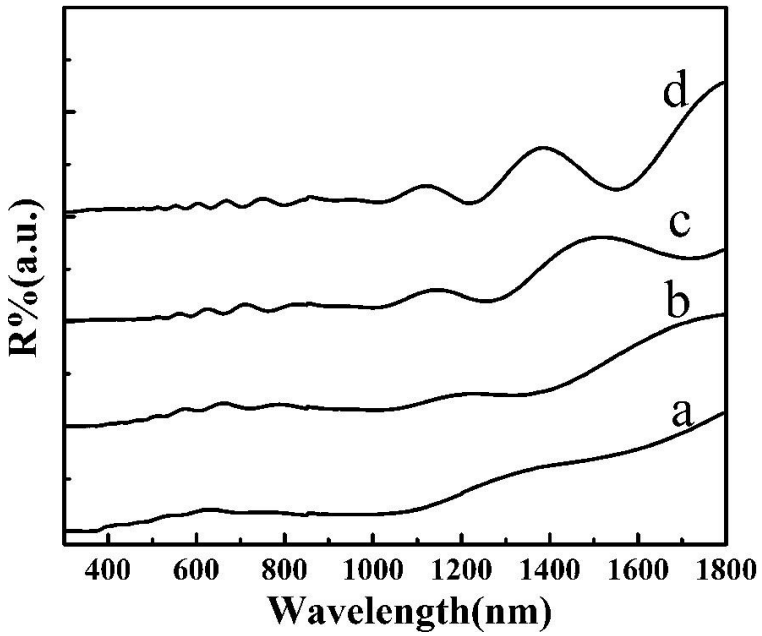

Figure 2.4 Reflection spectra of ZnO nanorod films prepared at different growth times: (a)0.5 h, (b) 1 h, (c) 2.5 h and (d) 3 h. (Zheng et al., 2018)

To know the film thickness variation, the authors have estimated the film thickness by using the principle of interference extinction, which is based on the reflection of incident monochromatic parallel light on the upper and lower surfaces of the film as shown in Figure 2.5.

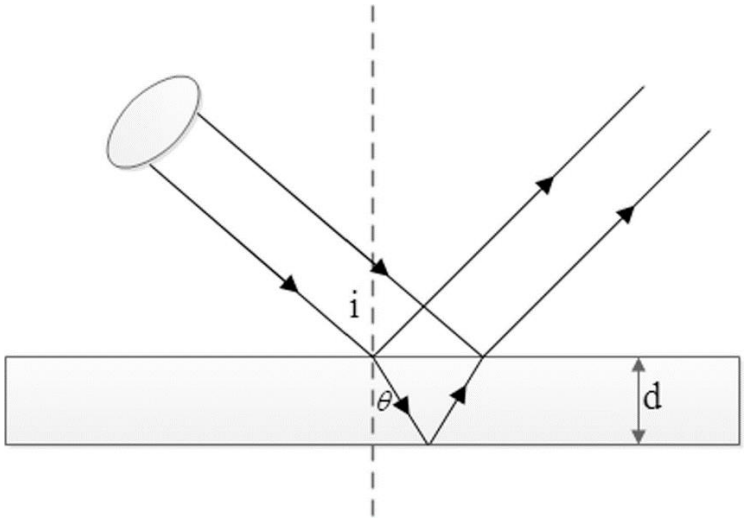

Figure 2.5 Principle of measuring film thickness in reflection mode. (Zheng et al., 2018)

Using a broadband light source in combination with a spectrophotometer to scan the wavelength of incident light, to get the reflected light with alternating intensities, and the interference extinction and interference enhancement phenomena occurred on the surface of the film, respectively. According to the following calculation formula, the thickness of thin film can be calculated, as shown in Table 2.1.

$$d = \frac{1}{2\sqrt{n^2 - \sin^2\varphi}} \cdot \frac{\lambda_1 \times \lambda_2}{\lambda_1 - \lambda_2} \cdot \frac{p}{1000} = \frac{1}{2\sqrt{n^2 - \sin^2\varphi}} \cdot \frac{p}{r_1 - r_2} \cdot 10^4[\mu m] \quad (2.1)$$

where λ_1 and λ_2 are the wavelength (nm) of the interference peak, r_1 and r_2 are wave numbers (cm^{-1}) of λ_1 and λ_2 respectively, and p is the number of interference peaks between λ_1 and λ_2. It is determined by the software itself. The refractive index n is 2.00 which is the refractive index of the bulk ZnO. The incident angle φ is zero.

Table 2.1 Film thickness of ZnO films with different growth times. (Zheng et al., 2018)

Growth time (h)	**Film thickness (μm)**
0.5	0.393
1	0.896
2.5	1.516
3	1.757

The authors compared the film thickness of 3 h measured by SEM with its calculated value, and found that the error is 4.6%, which indicates that the reflection mode method to estimate the film thickness of ZnO nanorod arrays is reliable.

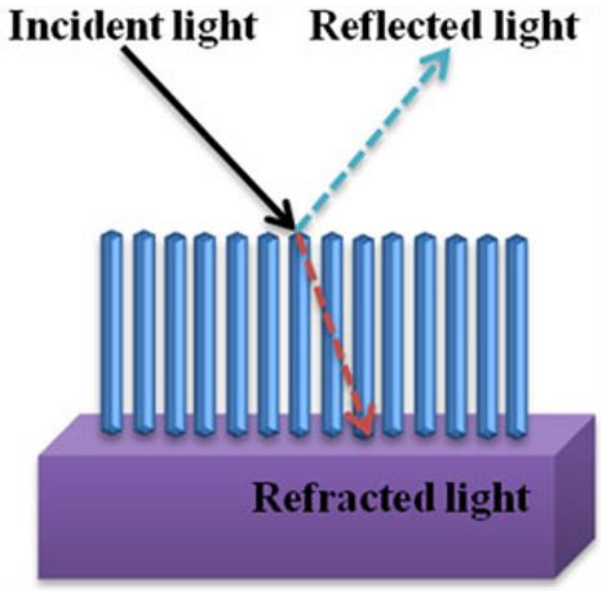

Figure 2.6 Schematic diagram of the nanorods light path (Baek et al., 2012).

P.F. Azad et.al reported the growth of ZnO nanorods on p-type silicon (100) wafer substrates by CBD method. The authors investigated the structural, morphological and optical properties of ZnO nanorods (Fallah Azad et al., 2017). The ZnO seed layer was deposited by RF magnetron sputtering method. The aqueous solution for chemical bath was prepared by zinc acetate dihydrate ($Zn((O_2CCH_3)_2(H_2O)_2)$) and ammonia hydroxide (NH_4OH) in 1:10 by volume. The deposition duration was 120 min, and the temperature of the solution was kept at 85°C.

Figure 2.7 shows the FESEM images of ZnO nanorods. It can be seen that the ZnO nanorods are distributed uniformly and densely from the surface view, the cross-section shows that nanorods are grown vertically on the seed layer. The length of ZnO nanorods is 61.27 nm and the diameter is 1.22 μm. Figure 2.8 shows the XRD pattern of ZnO nanorods grown on P-type silicon. The (002) crystal plane is the dominant peak, so the ZnO nanostructures grow with this orientation. The average crystallite size of the ZnO nanostructures is ~57 nm.

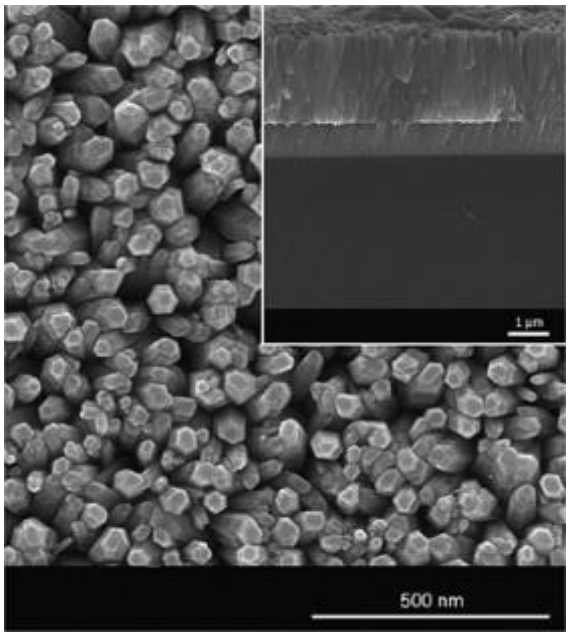

Figure 2.7 FE-SEM of ZnO nanorods deposited on ZnO/Si substrate. Inset is a cross-sectional view. (Fallah Azad et al., 2017)

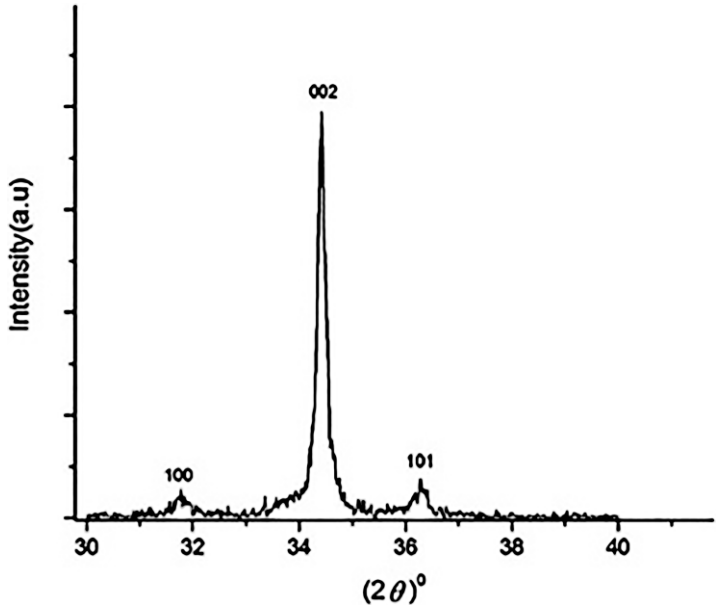

Figure 2.8 XRD pattern of ZnO nanorods which were grown on ZnO seed layer using CBD technique. (Fallah Azad et al., 2017)

Figure 2.9 shows the light reflectance of bare silicon, ZnO seed layer deposited by RF sputtering and ZnO nanorods grown by CBD. The bare silicon wafer has the highest light reflectance as can be seen from the comparison results. The ZnO nanorods grown by CBD show low reflectance mainly in the visible region, which is important for solar cell applications. Figure 2.10 shows the photoluminescence (PL) spectra at room temperature of the ZnO seed layer deposited by RF sputtering and the ZnO nanorods

grown by chemical bath deposition. Both samples have two emission peaks. The two peaks for the ZnO seed layer are at 382 and 556 nm. For the ZnO nanorods, the two peaks are at 379 and 554 nm, respectively. The intensity of the PL peaks is determined by the number of free excitons. The broad peaks appearing in the 500-700 nm region are associated with the deep-level emission of ZnO bandgap, which is due to specific defects such as oxygen vacancies and zinc interstitials. The intensity ratio of the UV and visible peaks of the ZnO seed layer and the grown ZnO nanorods is 43.75 and 13.49, respectively, which is influenced by the number of resident defects in the ZnO crystal. The above results indicate that the ZnO seed layer facilitates the nucleation of ZnO nanorods and improves the uniformity of synthesized ZnO nanorods.

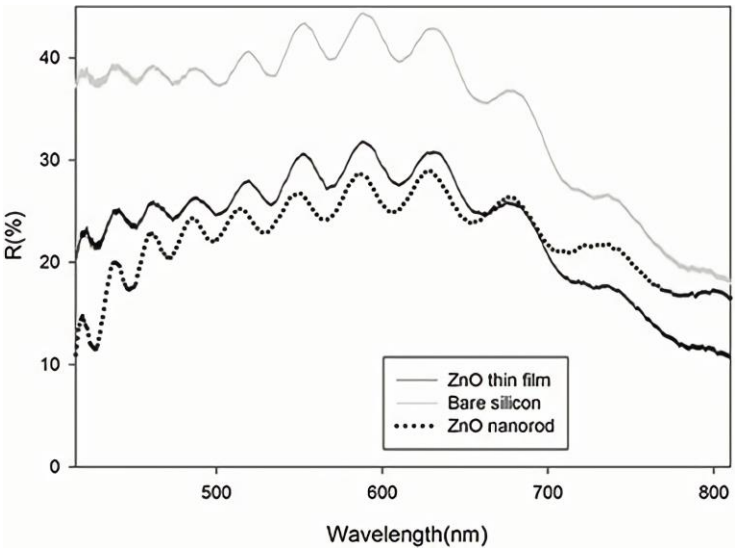

Figure 2.9 Light reflectance spectra from polished silicon surface, ZnO thin film, and ZnO nanorods. (Fallah Azad et al., 2017)

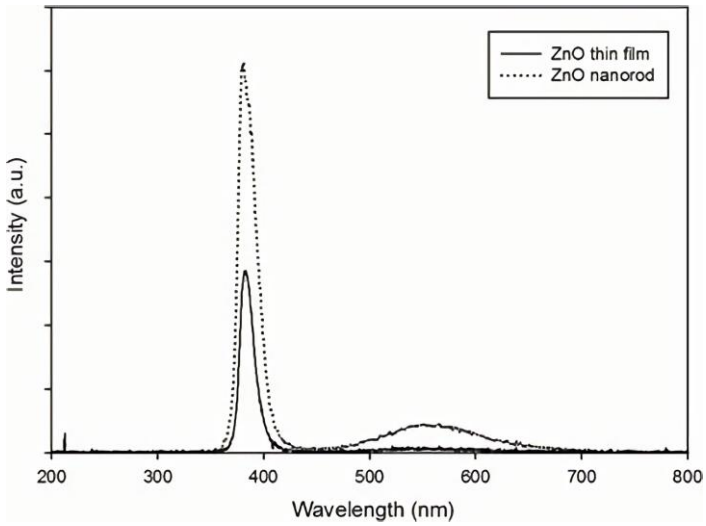

Figure 2.10 Room-temperature PL spectra for ZnO nanorod arrays and ZnO thin film on silicon substrates. (Fallah Azad et al., 2017)

With regard to the effect of CBD method growth time on the different properties of semiconductor materials, many scholars have also reported. H. S. Wai and C. Li systematically studied the growth of well-aligned ZnO nanorods using the CBD method, focusing on how reaction time influences structural, optical, and photocatalytic properties (Wai & Li, 2023). The ZnO nanorods were vertically grown on aluminum-doped ZnO (AZO) seed layers deposited by RF sputtering. The CBD process was kept at 95 °C using a mixed precursor solution of 0.015 mol/L $Zn(NO_3)_2 \cdot 6H_2O$ and 0.0075 mol/L HMTA, with growth durations ranging from 1 to 5 h at 1-hour intervals.

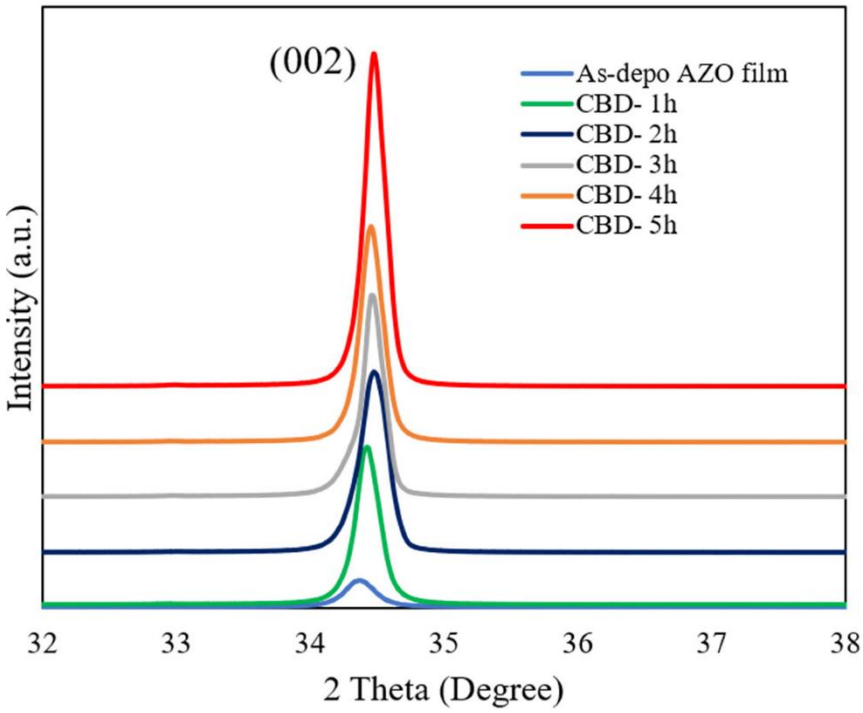

Figure 2.11 GIXRD patterns of ZnO nanorods with different reaction times by CBD method. (Wai & Li, 2023)

Figure 2.11 presents the XRD patterns of the as-deposited AZO film and the ZnO nanorods grown on the AZO seed layer by CBD method. Structurally, the ZnO nanorods exhibit a strong preferred growth orientation along the (0001) c-axis direction matching with the crystallographic orientation of the AZO seed layer. The crystallinity of the ZnO nanorods significantly improves with increasing reaction time: the crystallite size increases from 30.2 nm to 39.5 nm, while the FWHM decreases and the (002) peak intensity increases. The compressive stress decreases over growth time from -0.95 GPa to +0.47 GPa, indicating the compressive stress was gradually relieved in ZnO nanorods grown by the CBD process. Additionally, the lattice mismatch between the ZnO nanorods and the AZO thin film decreases from 0.09% to 0.06% with increased growth time, signifying enhanced lattice matching between the ZnO nanorods and the AZO seed layer. Table 2.2 summarizes the data obtained from XRD analysis.

Table 2.2 XRD analysis date of as-deposited AZO film and ZnO nanorods. (Wai & Li, 2023)

Samples	Peak Position (Deg)	Intensity (a.u.)	FWHM (Deg)	d (nm)	C-axis Crystallite Size (nm)	Lattice Constant, c (nm)	Stress (GPa)
As-depo AZO film	34.32	9821	0.384	2.6098	21.2	0.52	−1.185
CBD-1 h	34.36	21542	0.272	2.6085	30.2	0.52	−0.95
CBD-2 h	34.39	37403	0.258	2.6077	31.8	0.52	−0.82
CBD-3 h	34.41	40043	0.251	2.6051	32.7	0.52	−0.37
CBD-4 h	34.42	58367	0.242	2.6021	34.1	0.52	0.15
CBD-5 h	34.45	81245	0.208	2.6003	39.5	0.52	0.47

Figure 2.12 shows SEM images of the as-deposited AZO film and the ZnO nanorods grown on AZO seed layer using the CBD method at different reaction times. The plan view shows that the ZnO nanorods exhibit well-defined hexagonal facets. As the reaction time increases, the nanorod diameter increases slightly from 51 nm to 97 nm, while their density decreases significantly from 310/μm² to 88/μm². The cross-sectional views indicate that the average length of the ZnO nanorods increases significantly from 144 nm at 1 h to 1300 nm at 5 h. Furthermore, the preferential orientation of the nanorods improves with the extension of growth time.

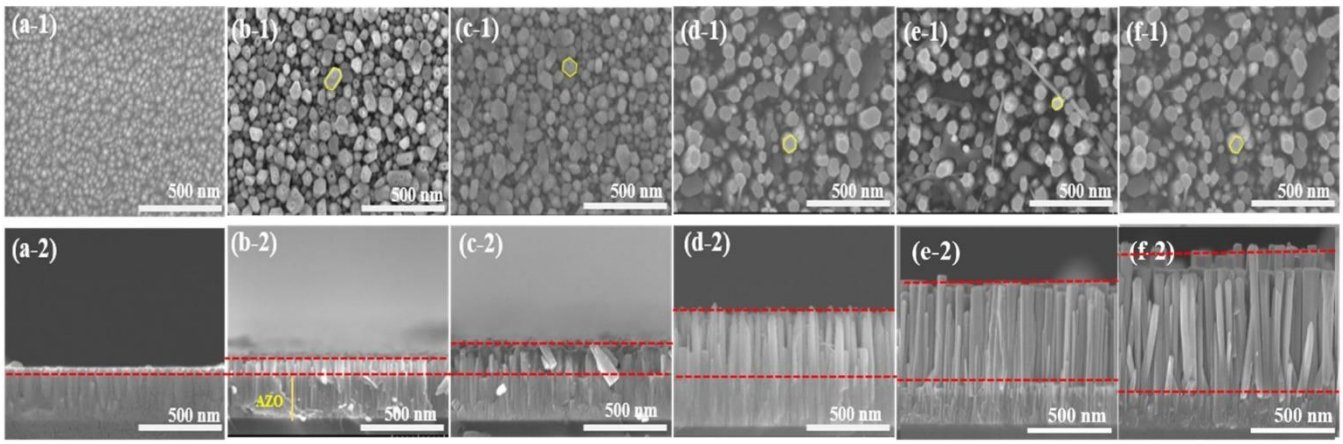

Figure 2.12 SEM images of ZnO nanorods with diffraction reaction times by CBD method: top views (a-1) as-deposited AZO film, (b-1) CBD—1 h, (c-1) CBD—2 h, (d-1) CBD—3 h, (e-1) CBD—4 h, and (f-1) CBD—5 h; cross-section views: (a-2) as-deposited AZO film, (b-2) CBD—1 h, (c-2) CBD—2 h, (d-2) CBD—3 h, (e-2) CBD—4 h, and (f-2) CBD—5 h. (Wai & Li, 2023)

Longer reaction times allowed more Zn^{2+} ions (from $Zn(NO_3)_2$) and OH^- ions (from HMTA) to react, forming more $Zn(OH)_2$ which dehydrated to ZnO. These crystallites stacked preferentially along the c-axis, increasing nanorod length. The Energy Dispersive X-ray (EDX) analysis, as shown in Figure 2.13, confirms that the Zn/O atomic ratio increases with the growth time in the CBD process, further supporting the formation of ZnO nanorods.

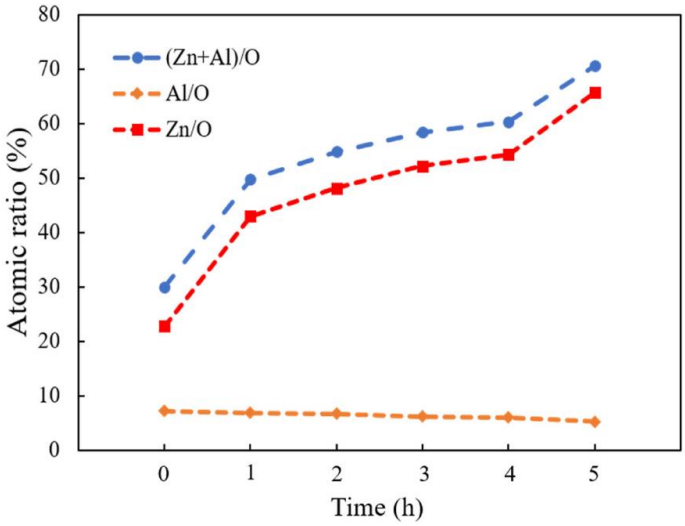

Figure 2.13 Variations of (Zn + Al)/O, Zn/O, and Al/O atomic ratios calculated from EDX analysis of as-deposited AZO film and ZnO nanorods with different reaction times by CBD method. (Wai & Li, 2023)

Figure 2.14 shows the optical transmittance spectra of the as‐deposited AZO film and ZnO nanorods on the as-deposited AZO film with different reaction times. The optical transmittance in the visible region remained high (>70%) for all samples. As the growth time increased, the optical band gap of the ZnO nanorods decreased slightly from 3.31 eV to 3.21 eV, attributed to improved crystallinity and reduced defects. The narrowed bandgap facilitated electron transfer from the valence to conduction band, thereby enhancing charge carrier generation and active radical formation. This mechanism ultimately improved the photocatalytic degradation efficiency.

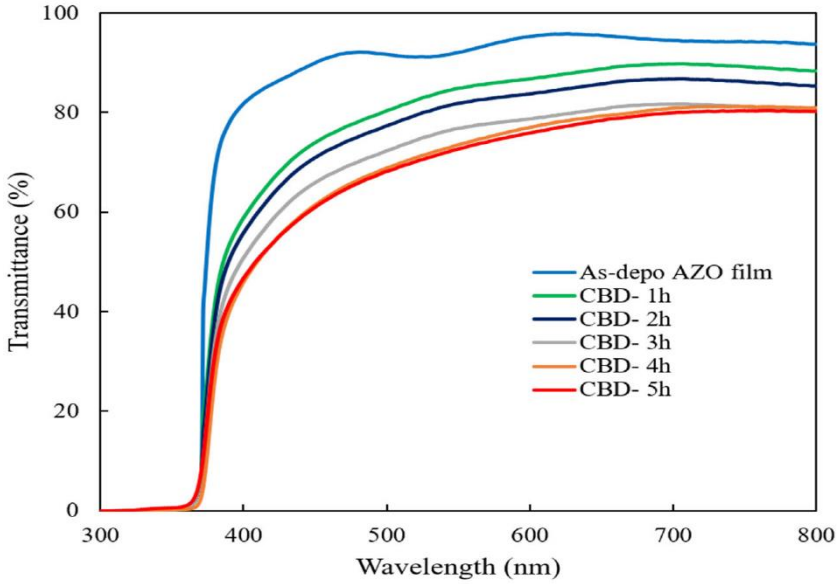

Figure 2.14 Optical transmittance spectra of ZnO nanorods with different reaction times by CBD method. (Wai & Li, 2023)

The photocatalytic activity of ZnO nanorods was assessed by monitoring the degradation of Methyl Red (MR) dye under UV light irradiation. As shown in Figure 2.15(a) and (b), ZnO nanorods grown for 5 hours exhibited the lowest absorption intensity and residual MR concentration, indicating the highest photocatalytic efficiency. The pseudo-first-order reaction rate of the ZnO nanorods increased from 0.0021 min^{-1} to 0.0057 min^{-1} with extended growth time, confirming the enhancement of

photocatalytic efficiency. This improvement is attributed to the increased volume (including the length and diameter) of the ZnO nanorods, which provides more active sites for photocatalytic reactions. The increase in the number of active sites enhances the surface absorption ability for the MR molecules while improving incident photon capture. This process generates photogenerated charge carriers, thereby accelerating the degradation reaction rate.

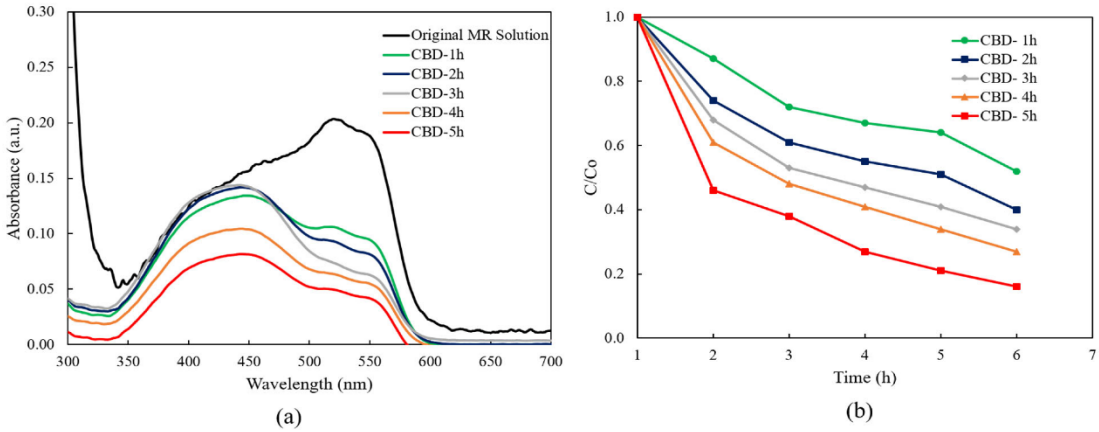

Figure 2.15 (a) The absorption spectra of MR solution for ZnO nanorods with different reaction times and (b) plot of C/C_0 versus the degradation reaction time. (Wai & Li, 2023)

S. Kumar et al. synthesized ZnO–SiO_2 nanocomposite thin films under alkaline conditions (pH = 10.8) at 90 °C by CBD method, discussing the effect of deposition time (20, 40, 60 and 120 min) on structural, morphological, optical, and electrical properties of ZnO–SiO_2 thin films (Kumar et al., 2021).

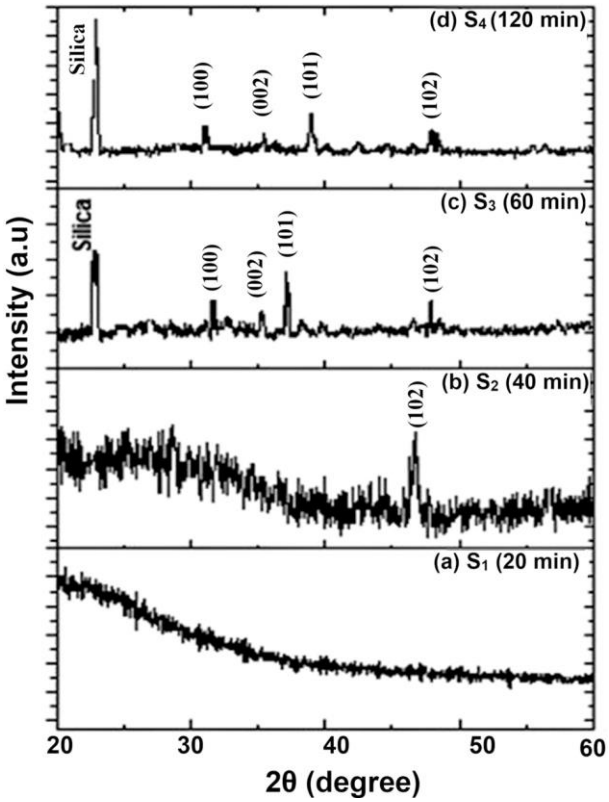

Figure 2.16 XRD of ZnO-SiO_2 nanocomposite for growth periods of (a) 20min (b) 40 min (c) 60 min (d) 120 min. (Kumar et al., 2021)

Figure 2.16 showed the XRD patterns of ZnO-SiO_2 nanocomposite for different growth duration. Films deposited for 20 and 40 min exhibited an amorphous phase. While the ZnO–SiO_2 indicated crystalline and composite structure with longer durations (60 and 120 min). The intensity of the (002) peak which is the ZnO characteristic peak decreased due to the presence of silica. The (002) peak showed the minimum intensity may be due to the distortion of the ZnO lattice in the presence of silica.

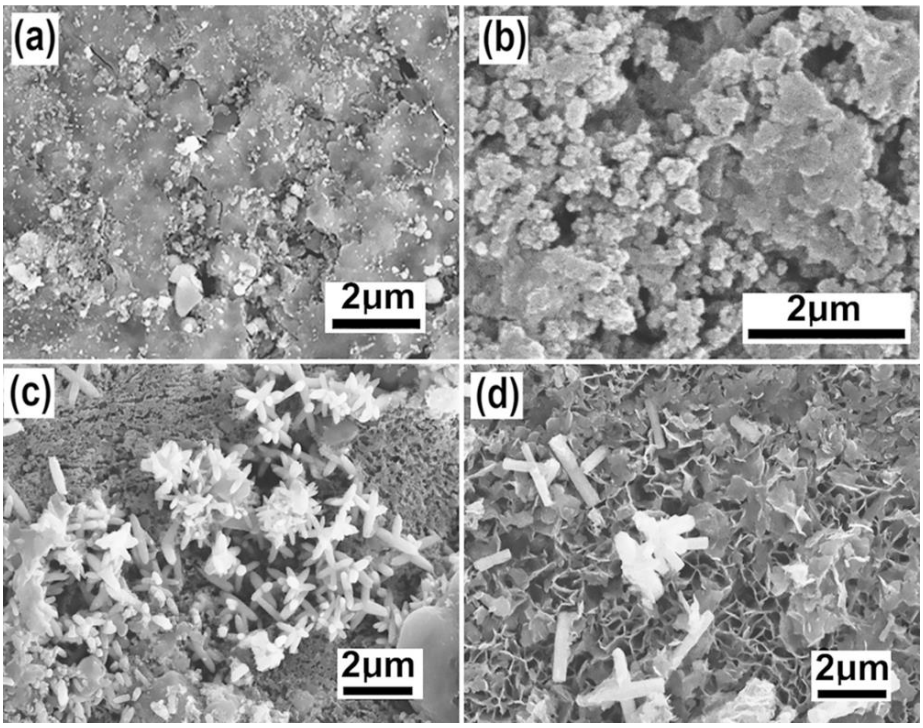

Figure 2.17 SEM Image of ZnO-SiO2 nanocomposite thin film for a growth period of (a) 20 min, (b) 40 min, (c) 60 min, (d) 120 min. (Kumar et al., 2021)

Figure 2.17 is the SEM image of ZnO-SiO_2 nanocomposite thin film for different growth times. The film formed thin sheets with good coverage, which grown at 20 min. But the films grown at 40 min indicated closely scattered agglomerates. With the growth time increased to 60 min, the dispersion of nanoparticles is due to the thin layer of SiO_2 covering the ZnO surface. Uuniform porous films oriented normal to the substrate were obtained at 120 min growth time.

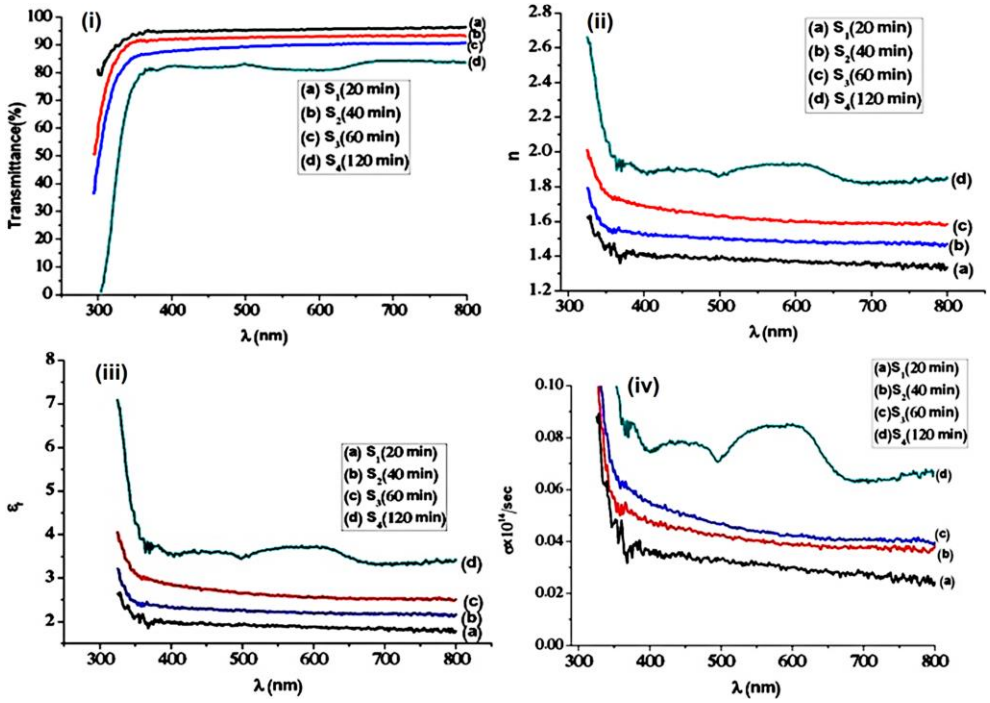

Figure 2.18 (i) Transmittance (ii) Refractive Indices (iii) Dielectric constants and (iv) Optical conductivities of ZnO-SiO2 nanocomposite thin films deposited at different deposition durations. (Kumar et al., 2021)

Figure 2.18 (i) shows the transmittance of ZnO-SiO_2 nanocomposite thin films deposited at different deposition durations. As the growth time increased, the transmittance of the ZnO-SiO_2 films decreased at 500 nm due to the increase in film thickness and grain boundary scattering. The film grown at 120 min had the highest refractive index, dielectric constant, and optical conductivity, as shown in Figure 2.18 (ii), (iii) and (iv), which was associated with the thickest film. The ZnO-SiO_2 films thickness calculated by the equation:

$$t = \frac{m}{A\rho} \tag{2.2}$$

where m is the mass of the film deposited on area A and the value of ρ was observed to be 4.9 g·cm^{-3} (Vijayan et al., 2008).